Translational Oncology 56 (2025) 102395

Contents lists available at ScienceDirect

Translational Oncology

journal homepage: www.elsevier.com/locate/tranon

Original Research

N6-methyladenosine binding protein YTHDF2 inhibits gastric cancer cell growth and predicts better prognosis in patients with gastric cancer

Jun Zheng [a,1], Yinhua Liang [a,1], Xin Xu [b], Jianpeng Zhou [a], Shuang Jiang [a], Jiwei Yu [a,*]

[a] Department of General Surgery, Shanghai Ninth People's Hospital, School of Medicine, Shanghai Jiao Tong University, Shanghai, PR China
[b] Department of Neurosurgery, Shanghai Ninth People's Hospital, School of Medicine, Shanghai Jiao Tong University, Shanghai, PR China

ARTICLE INFO

Keywords:
Gastric cancer
YTH N6-methyladenosine RNA binding protein 2 (YTHDF2)
The Cancer Genome Atlas (TCGA)
Gastric cancer cell growth
Prognosis

ABSTRACT

Background: The potential role of N6-methyladenosine (m6A) in cancer progression has received significant attention in the past few years. The purpose of this study aimed to evaluate the impact of YTH N6-methyladenosine RNA-binding protein 2 (YTHDF2) on patient prognosis and its potential role in gastric cancer.
Methods: A total of 305 patients with clinically informative gastric cancer were identified from The Cancer Genome Atlas (TCGA) dataset, and GSE29272 and GSE84437 were used as external validation. Different m6A modulators were analyzed using the Limma package; the Cox regression models were used to determine risk factors for overall survival (OS). A 1:1 propensity score matching (PSM) analysis was used to adjust for differences in baseline clinicopathological characteristics between the YTHDF2 low and high expression groups. The Cox regression analysis was then used to identify risk factors for OS. Gene ontology (GO) and Kyoto Encyclopedia of Genes and Genomes (KEGG) analyses were used to explore the potential role and function of YTHDF2 in gastric cancer. And the effects of YTHDF2 on the growth of gastric cancer cells were detected in vivo and in vitro.
Results: Nineteen m6A methylation regulators were expressed in gastric cancer tissues; YTHDF2 was associated with the prognosis of gastric cancer patients. The expression level of YTHDF2, patient age, and tumor stage were independent risk factors for OS. After PSM, YTHDF2 expression led to a relatively better prognosis and staging. Patients in stage IV had a significantly worse prognosis. The expression of YTHDF2 was associated with cancer-related functions and pathways in gastric cancer. We found that YTHDF2 has lower expression in gastric cancer cells and inhibits the growth of GC cells.
Conclusions: The high expression of YTHDF2 can predict a better prognosis of gastric cancer patients. YTHDF2 exerts a critical role in gastric cancer progression by inhibiting the growth of GC cells.

Introduction

Gastric cancer (GC) remains a prevalent malignancy and ranks as the third leading cause of cancer-related mortality worldwide [1]. Due to the absence of early symptoms, most patients are diagnosed at an advanced stage, often accompanied by rapid progression and metastasis, leading to poor clinical outcomes [2]. The lack of precise prognostic markers and targeted therapeutic strategies necessitates a deeper understanding of GC pathogenesis to improve survival predictions and therapeutic interventions. Identifying reliable prognostic biomarkers and elucidating their molecular mechanisms may facilitate the development of novel treatment strategies to enhance patient outcomes.

N6-methyladenosine (m6A), the most prevalent internal modification in eukaryotic mRNA, has emerged as a critical epigenetic regulator in tumorigenesis [3]. The m6A modification is dynamically regulated by methyltransferases ("writers"), demethylases ("erasers"), and m6A-binding proteins ("readers") [4,5]. Among these, YTH domain-containing proteins function as key readers that mediate m6A-dependent RNA processing [6,7]. YTH N6-methyladenosine RNA binding protein 2 (YTHDF2), a major m6A reader, predominantly

Abbreviations: GC, Gastric Cancer; YTHDF2, YTH N6-methyladenosine RNA binding protein 2; TCGA, the Cancer Genome Atlas; m6A, N6-methyladenosine; OS, Overall survival; FTO, Fat Mass and Obesity Associated Gene; PSM, Propensity score matching; GO, Gene Oncology; KEGG, Kyoto Encyclopedia of Genes and Genomes; SD, the standard difference; SPSS, Statistical Product and Service Solutions; HR, Hazard ratios; CI, Confidence interval; MSS, Microsatellite stability; MSI-L, Microsatellite instability-Low; MSI-H, Microsatellite instability-High; EMT, Epithelial-mesenchymal transition; GEO, Gene Expression Omnibus.

* Corresponding author.
E-mail addresses: jenniferyu919@126.com, jenniferyu0919@sjtu.edu.cn (J. Yu).

[1] Jun Zheng and Yinhua Liang contributed equally to this study.

https://doi.org/10.1016/j.tranon.2025.102395
Received 17 October 2024; Received in revised form 8 March 2025; Accepted 7 April 2025

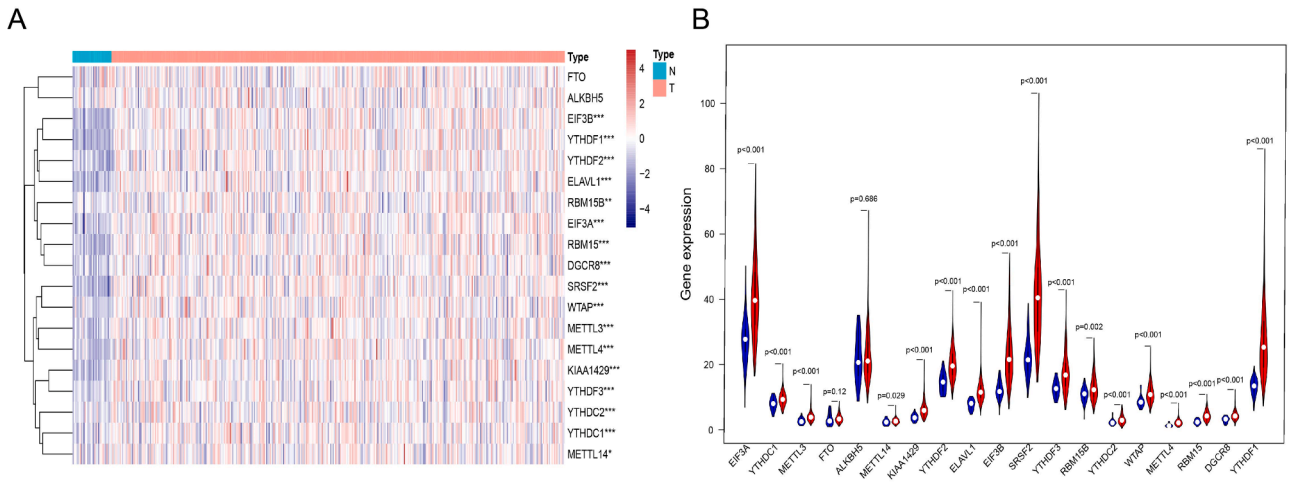

Fig. 1. The expression level of m6A RNA methylation regulators. **(A)** Expression differences of m6A RNA methylation regulators in gastric cancer based on TCGA data. Red and blue represent the relatively high or low expression, respectively. $^{*}p < 0.05$, $^{**}p < 0.01$, $^{***}p < 0.001$. **(B)** Vioplot visualizing the differentially m6A RNA methylation regulators in gastric cancer (blue is normal and red is gastric cancer).

facilitates mRNA degradation by recognizing m6A modifications in the 3′-UTR, while it can also enhance protein translation when binding to the 5′-UTR [8]. The role of YTHDF2 in cancer is context-dependent. In GC, YTHDF2 has been reported to promote LINC00470-METTL3-mediated PTEN mRNA degradation, influencing tumor progression [9]. Its knockdown suppresses proliferation and induces apoptosis in GC cell lines [10]. Additionally, YTHDF2 regulates epithelial-mesenchymal transition in pancreatic cancer via the YAP signaling pathway [11] and modulates hepatocellular carcinoma growth by destabilizing ERGF mRNA [12]. Despite these findings, the precise function of YTHDF2 in GC and its prognostic significance remain unclear.

In this study, we investigated the impact of YTHDF2 on GC prognosis through bioinformatics analyses and functional validation. Our findings suggest that YTHDF2 plays a pivotal role in GC progression and may serve as a potential biomarker for risk assessment and therapeutic targeting.

Methods

Data source and acquisition

The expression profiles of GC and normal tissues were retrieved from The Cancer Genome Atlas (TCGA) (https://portal.gdc.cancer.gov). Clinical annotations were obtained from the UCSC Xena database (http://xena.ucsc.edu). A total of 375 GC tumor samples and 32 normal gastric tissues were included in the analysis. After filtering for cases with complete clinical information, 305 GC patients were retained for survival analysis. Gene expression values were normalized using $\log_2(\text{FPKM} + 1)$ transformation.

To validate the differential expression of YTHDF2 between tumor and normal tissues, we incorporated the GSE29272 dataset from the Gene Expression Omnibus (GEO) (https://www.ncbi.nlm.nih.gov/geo/). This dataset includes 30 adjacent normal tissues and 134 GC tumor samples, providing an additional independent cohort for expression validation. Furthermore, we employed GSE84437, a microarray dataset containing 433 GC patients with gene expression and survival data, as an external validation cohort to assess the prognostic significance of YTHDF2.

m6A methylation regulators

Based on previously published studies, we identified 23 key m6A methylation regulators for screening potential prognostic factors in GC. These include seven m6A writers (KIAA1429, METTL14, METTL3, METTL4, RBM15, RBM15B, WTAP), fourteen m6A readers (DGCR8, EIF3A, EIF3B, ELAVL1, HNRNPA2, HNRNPB1, HNRNPC1, HNRNPC2, SRSF2, YTHDC1, YTHDC2, YTHDF1, YTHDF2, YTHDF3), and two m6A erasers (ALKBH5, FTO).

Data process

To ensure the robustness of survival analysis and minimize potential confounding effects, propensity score matching (PSM) was applied to balance clinicopathological characteristics between the low- and high-YTHDF2 expression groups. Using the "MatchIt" package in R, we performed 1:1 nearest neighbor matching with a caliper width of 0.1 to optimize comparability between the two groups. The matching process incorporated the following baseline variables: age, gender, tumor stage, T/N/M classification, histological grade, and molecular subtype (MSS, MSI-L, MSI-H).

To assess the effectiveness of PSM, we calculated standardized mean differences (SMDs) for each covariate before and after matching, considering SMD < 0.2 as indicative of a well-balanced cohort. After matching, 212 patients were included in the final analysis. Sensitivity analysis was conducted by comparing results obtained from 1:1 and 1:2 matching strategies to ensure consistency in prognostic assessments.

Following PSM, Cox regression analysis was performed to identify independent prognostic factors associated with overall survival (OS) in matched cohorts. Kaplan-Meier survival curves with log-rank tests were used to compare OS between the low- and high-YTHDF2 expression groups, with statistical significance set at $P < 0.05$.

Cell culture

Gastric cancer cell lines (HGC27, MKN28, SGC-7901, and AGS) and the normal gastric epithelial cell line (GES-1) were obtained from the Cell Bank of Fudan University. Cells were cultured in Dulbecco's Modified Eagle's Medium (DMEM) supplemented with 10 % fetal bovine serum (FBS), 100 U/mL penicillin G, and 100 μg/mL streptomycin sulfate (BasalMedia, Cat# E210702). All cell lines were maintained at 37 °C in a humidified incubator with 5 % CO_2 and were passaged for no more than three months post-resuscitation to ensure cellular integrity.

RNA extraction, reverse transcription, and quantitative PCR (RT-qPCR)

Total RNA was extracted from GC cells and tissues using Trizol reagent (Invitrogen, USA). RNA concentration and purity were

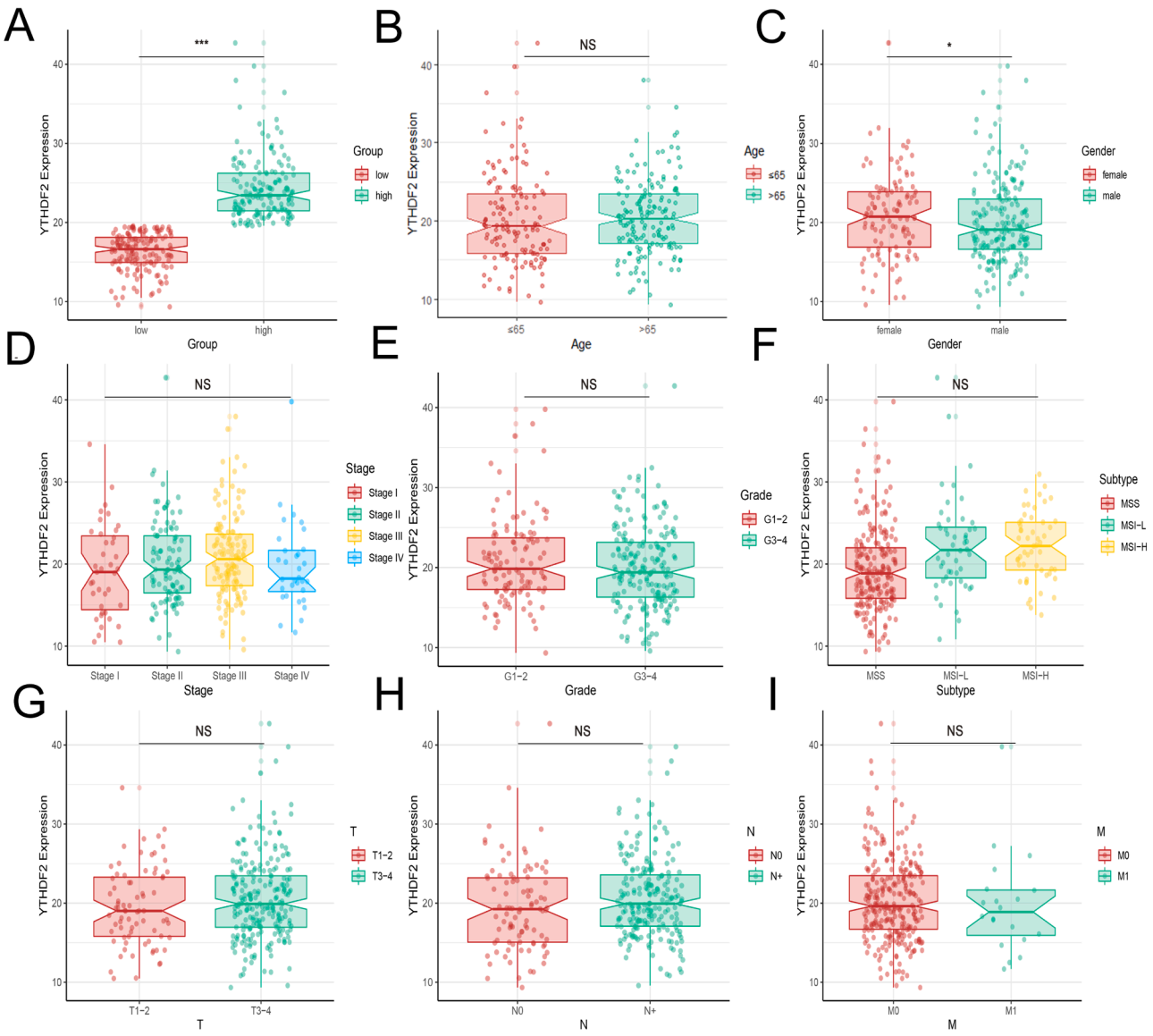

Fig. 2. Analysis of YTHDF2 expression in patients with different baseline clinicopathological characteristics. **(A)** Patients were divided into low and high expression groups according to the expression level of YTHDF2. **(B-I)** Differences of YTHDF2 expression among age, gender, stage, grade, subtype, T, N, and M groups. *$p < 0.05$, NS means no significance.

determined using a NanoDrop2000 spectrophotometer (NanoDrop Technologies Inc., Wilmington, USA). Complementary DNA (cDNA) was synthesized with a reverse transcription kit following the manufacturer's protocol.

RT-qPCR was performed to quantify YTHDF2 mRNA expression, using glyceraldehyde-3-phosphate dehydrogenase (GAPDH) as an internal control. The primer sequences for YTHDF2 were as follows:

Forward: 5′- ATAGTTTGCCTCCAGCCACC −3′

Reverse: 5′- GGACCGAAGCTTCTCCAACA −3′

Relative gene expression levels were calculated using the $2^{-\Delta\Delta}$Ct method.

Plasmid transfection and gene knockdown

Stable YTHDF2 overexpression was established using lentiviral vectors constructed by Obio Technology (Shanghai, China). Short hairpin RNAs (shRNAs) specifically targeting YTHDF2 were synthesized and cloned into lentiviral vectors by Obio Technology for gene knockdown experiments.

Transient transfections of expression plasmids were performed using Lipofectamine 3000 (Invitrogen, USA) according to the manufacturer's instructions. Cells were harvested 48 h post-transfection for subsequent assays.

Western blotting

Protein extraction was performed using radioimmunoprecipitation assay (RIPA) lysis buffer supplemented with phenylmethanesulfonyl fluoride (PMSF) protease inhibitor (100:1, Beyotime, Shanghai, China). Protein concentrations were measured using a Bicinchoninic Acid (BCA) Protein Assay Kit (Beyotime, Shanghai, China).

Equal amounts of protein were separated via SDS-PAGE and transferred onto polyvinylidene fluoride (PVDF) membranes (Millipore, USA). Membranes were blocked with 5 % skimmed milk, followed by overnight incubation with primary antibodies at 4 °C. After washing with Tris-buffered saline with Tween 20 (TBST), membranes were incubated with secondary antibodies (Abcam, USA) at room temperature for 2 h. Protein bands were visualized using enhanced chemiluminescence (ECL) reagent (Beyotime, Shanghai, China). The expression levels of target proteins were quantified by normalizing the

Table 1
Baseline clinicopathological characteristics.

Variables	Total (*N* = 305)	YTHDF2 Low (*N* = 152)	YTHDF2 High (*N* = 153)	P value
Age, n (%)				0.122
≤65	139 (45.6)	76 (24.9)	63 (20.7)	
>65	166 (54.4)	76 (24.9)	90 (29.5)	
Gender, n (%)				0.049
female	113 (37.0)	48 (15.7)	65 (21.3)	
male	192 (63.0)	104 (34.1)	88 (28.9)	
Stage, n (%)				0.287
Stage I	39 (12.8)	22 (7.2)	17 (5.6)	
Stage II	99 (32.5)	53 (17.4)	46 (15.1)	
Stage III	135 (44.3)	59 (19.3)	76 (24.9)	
Stage IV	32 (10.5)	18 (5.9)	14 (4.6)	
Grade, n (%)				0.666
G1–2	112 (36.7)	54 (17.7)	58 (19.0)	
G3–4	193 (63.3)	98 (32.1)	95 (31.1)	
T, n (%)				0.219
T1–2	75 (24.6)	42 (13.8)	33 (10.8)	
T3–4	230 (75.4)	110 (36.1)	120 (39.3)	
M, n (%)				0.633
M0	285 (93.4)	141 (46.2)	144 (47.2)	
M1	20 (6.6)	11 (3.6)	9 (3.0)	
N, n (%)				0.098
N0	93 (30.5)	53 (17.4)	40 (13.1)	
N+	212 (69.5)	99 (32.5)	113 (37.0)	
Subtype, n (%)				<0.0001
MSS	204 (66.9)	119 (39.0)	85 (27.9)	
MSI-L	48 (15.7)	17 (5.6)	31 (10.2)	
MSI-H	53 (17.4)	16 (5.2)	37 (12.1)	

Table 2
Cox regression analysis of prognostic factors for overall survival in gastric cancer (GC).

	Univariate analysis		Multivariate analysis	
	HR[a] (95 % CI[b])	P	HR (95 % CI)	P value
YTHDF2 expression				
Low	Reference		Reference	
High	0.63 (0.42–0.95)	0.027	0.59 (0.39–0.89)	0.012
Age				
≤65	Reference		Reference	
>65	1.63 (1.08–2.46)	0.019	1.89 (1.24–2.88)	0.003
Gender				
female	Reference			
male	1.38 (0.89–2.12)	0.147		
Stage				
Stage I	Reference		Reference	
Stage II	1.78 (0.80–3.95)	0.156	1.82 (0.82–4.03)	0.138
Stage III	2.15(1.01–4.56)	0.047	2.32 (1.09–4.92)	0.029
Stage IV	3.70 (1.59–8.57)	0.002	4.23 (1.81–9.88)	<0.001
Grade				
G1–2	Reference			
G3–4	1.29 (0.86–1.95)	0.225		
T				
T1–2	Reference			
T3–4	1.51 (0.93–2.46)	0.096		
M				
M0	Reference			
M1	1.65 (0.80–3.40)	0.177		
N				
N0	Reference			
N+	1.43 (0.90–2.29)	0.130		
Subtype				
MSS[c]	Reference			
MSI-L[d]	1.40 (0.79–2.46)	0.246		
MSI-H[e]	0.73 (0.42–1.28)	0.278		

[a] HR: hazard ratio;.
[b] 95 % CI: 95 % confidence intervals;.
[c] MSS: microsatellite stability;.
[d] MSI-L: microsatellite instability-low;.
[e] MSI-H: microsatellite instability-high.

intensity of target bands to GAPDH. The primary antibody included anti-YTHDF2 (Abcam, ab19879) and anti-β-actin (Zhongshan Jinqiao, TA-08).

Wound healing assay

Cell migration ability was assessed using a wound healing assay. GC cells were seeded in 6-well plates and cultured until reaching 90 % confluence. A uniform scratch was introduced across the cell monolayer using a sterile pipette tip, after which the cells were maintained in serum-free medium. Images were captured at 0 h and 48 h using an inverted microscope in 10 randomly selected fields of view, and the migration distance was quantified to evaluate cell motility.

Transwell assay

The migration and invasion capacities of GC cells were evaluated using Transwell chambers with 8-μm pores (Corning Incorporated, USA). For the migration assay, 1×10^5 cells/mL were resuspended in serum-free medium, and 200 μL of the suspension was added to the upper chamber. The lower chamber was filled with 500 μL of DMEM containing 10 % FBS. After incubation at 37 °C with 5 % CO_2 for 24 h, migrated cells were fixed with methanol and stained with 0.5 % crystal violet (Beyotime, Shanghai, China).

For the invasion assay, the upper chambers were precoated with Matrigel matrix (BD Biosciences, USA) to simulate the extracellular matrix barrier. The experimental conditions and staining procedures were identical to those of the migration assay. Stained cells in five randomly selected fields were counted under a light microscope.

Animal studies

Animal experiments were conducted following protocols approved by the Institutional Animal Care and Use Committee (IACUC). Eight male BALB/c nude mice (4–6 weeks old, 20–25 g) were purchased from Shanghai JieSiJie Laboratory Animal Co., Ltd. (Shanghai, China). GC AGS cells were genetically modified to overexpress YTHDF2 (YTHDF2-oe) using lentiviral transduction. Cells transfected with an empty vector (oe-NC) served as controls.

A total of 5×10^7 cells/mL were suspended in PBS, and 0.2 mL of the suspension was injected subcutaneously into the left armpit of each mouse ($n = 4$ per group). Tumor growth was monitored and recorded at regular intervals. After two weeks, mice were euthanized by cervical dislocation, and tumors were excised and weighed for analysis.

Statistical analysis

All statistical analyses were performed using SPSS version 23.0 (SPSS Inc., Chicago, IL, USA) and R version 4.0.2 (The R Foundation for Statistical Computing, Vienna, Austria). Continuous variables were compared using the Student's *t*-test, while categorical variables were analyzed using the χ^2 test.

To identify independent prognostic factors for overall survival (OS), univariate and multivariate Cox regression analyses were conducted, with hazard ratios (HRs) and 95 % confidence intervals (CIs) reported. The Kaplan-Meier method was used to estimate survival curves, and differences between groups were assessed using the log-rank test. Statistical significance was set at $P < 0.05$.

Results

The m6A methylation regulators expression level in GC

To investigate the expression patterns of m6A methylation regulators in GC, we analyzed differentially expressed genes using transcriptomic data from 32 normal tissues and 375 tumor tissues in the TCGA

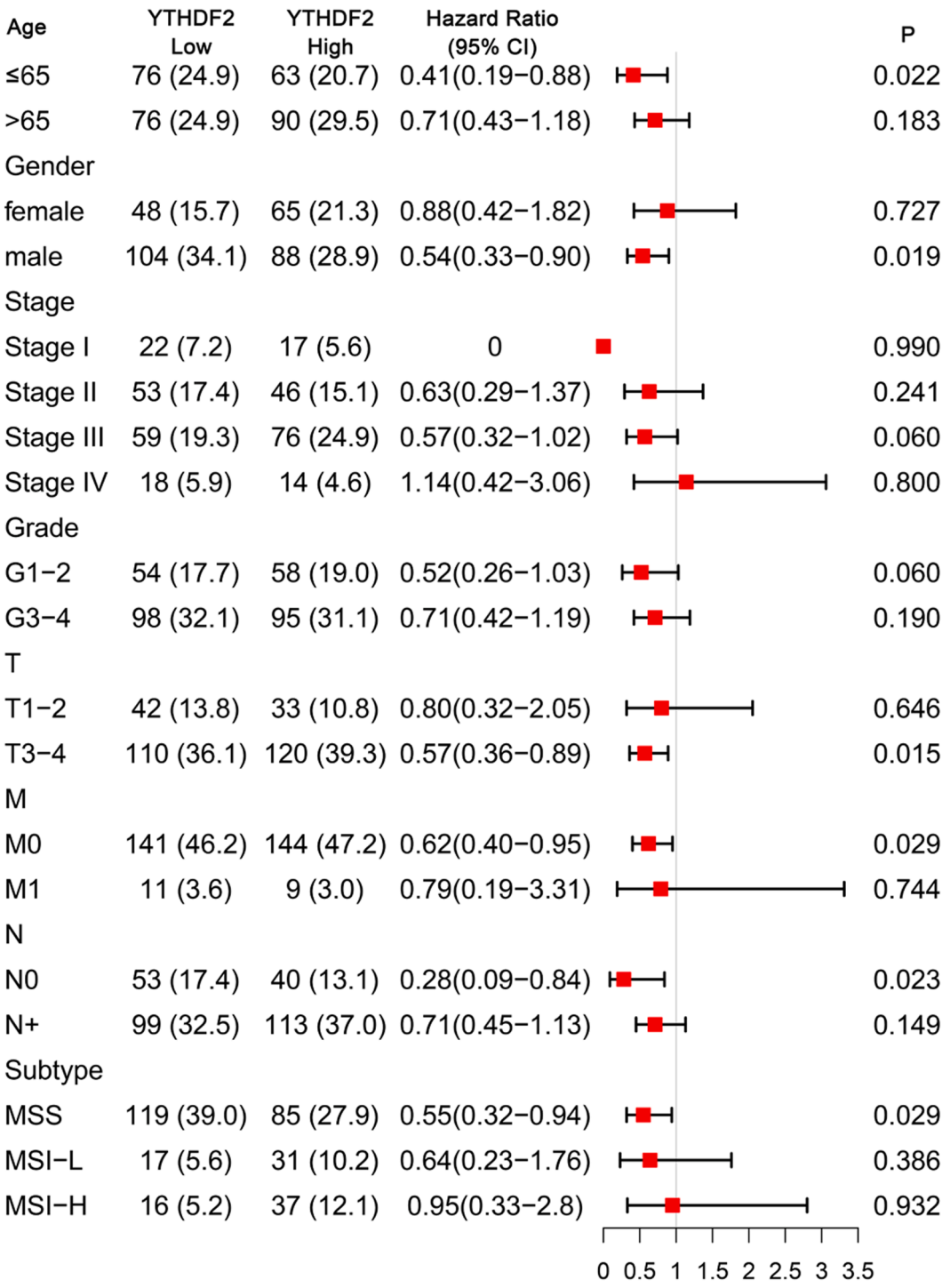

Fig. 3. Prognosis analysis in subtypes of each baseline clinicopathological characteristics group. The hazard ratios (HR) and 95 % confidence intervals (CI) were calculated by univariate Cox regression.

database. As shown in Fig. 1A and 1B, 19 out of 22 m6A regulators were expressed in GC, with 17 regulators significantly upregulated in tumor tissues compared to adjacent normal tissues.

Among these, m6A "writers" (KIAA1429, METTL14, METTL3, METTL4, RBM15, RBM15B, WTAP) and m6A "readers" (DGCR8, EIF3A, EIF3B, ELAVL1, SRSF2, YTHDC1, YTHDC2, YTHDF1, YTHDF2, YTHDF3) exhibited consistent overexpression in GC tissues. These findings suggest a potential role for m6A modification in GC pathogenesis.

The YTHDF2 expression level in baseline clinicopathological characteristics

To explore the prognostic relevance of m6A methylation regulators in GC, we conducted univariate Cox regression analysis on 19 regulators. The results identified YTHDF2, an m6A "reader", as a significant prognostic factor for overall survival (OS) (HR = 0.629, $P = 0.027$), suggesting a potential protective role in GC (see Supplementary File 1).

Based on YTHDF2 expression levels, GC patients were stratified into high- and low-expression groups (Fig. 2A). Further analysis integrating

Table 3
Propensity score matching (PSM) in gastric cancer (GC) patients based on YTHDF2 expression.

Variables	Before matching		SD[a]	After matching		SD
	Low (n = 152)	High (n = 153)		Low (n = 106)	High (n = 106)	
Age			0.178			0.095
≤65	76 (24.9)	63 (20.7)		49 (23.1)	44 (20.8)	
>65	76 (24.9)	90 (29.5)		57 (26.9)	62 (29.2)	
Gender			0.227			0.04
female	48 (15.7)	65 (21.3)		33 (15.6)	35 (16.5)	
male	104 (34.1)	88 (28.9)		73 (34.4)	71 (33.5)	
Stage			0.224			0.124
Stage I	22 (7.2)	17 (5.6)		11 (5.2)	14 (6.6)	
Stage II	53 (17.4)	46 (15.1)		35 (16.5)	34 (16.0)	
Stage III	59 (19.3)	76 (24.9)		48 (22.6)	49 (23.1)	
Stage IV	18 (5.9)	14 (4.6)		12 (5.7)	9 (4.2)	
Grade			0.049			<0.001
G1–2	54 (17.7)	58 (19.0)		38 (17.9)	38 (17.9)	
G3–4	98 (32.1)	95 (31.1)		68 (32.1)	68 (32.1)	
T			0.141			0.089
T1–2	42 (13.8)	33 (10.8)		23 (10.8)	27 (12.7)	
T3–4	110 (36.1)	120 (39.3)		83 (39.2)	79 (37.3)	
M			0.055			0.185
M0	141 (46.2)	144 (47.2)		96 (45.3)	101 (47.6)	
M1	11 (3.6)	9 (3.0)		10 (4.7)	5 (2.4)	
N			0.19			0.063
N0	53 (17.4)	40 (13.1)		29 (13.7)	32 (15.1)	
N+	99 (32.5)	113 (37.0)		77 (36.3)	74 (34.9)	
Subtype			0.502			0.12
MSS[b]	119 (39.0)	85 (27.9)		75 (35.4)	74 (34.9)	
MSI-L[c]	17 (5.6)	31 (10.2)		15 (7.1)	12 (5.7)	
MSI-H[d]	16 (5.2)	37 (12.1)		16 (7.5)	20 (9.4)	

[a] SD: Standard Deviation;.
[b] MSS: microsatellite stability;.
[c] MSI-L: microsatellite instability-low;.
[d] MSI-H: microsatellite instability-high.

baseline clinicopathological characteristics revealed that YTHDF2 expression was significantly higher in female patients compared to males, while no significant differences were observed among MSS, MSI-L, and MSI-H subtypes (Fig. 2B–I, Table 1).

We analyzed GSE29272, which includes 30 adjacent normal tissues and 134 tumor tissues, to validate the differential expression of YTHDF2 in GC. Consistently, YTHDF2 was significantly upregulated in tumor tissues, reinforcing its potential role in GC tumorigenesis (Supplementary file 2).

Risk factors of patient survival

Univariate and multivariate Cox regression analyses were performed using baseline clinicopathological characteristics to identify prognostic risk factors in GC. The results indicated that YTHDF2 expression, patient age, and tumor stage were significant predictors of OS (Table 2). Higher YTHDF2 expression was associated with improved OS, suggesting a potential protective role. In contrast, patients older than 65 years had a significantly higher risk of poor prognosis compared to those ≤65 years. Moreover, patients with stage III or IV disease exhibited an increased risk of mortality compared to those with stage I or II.

To further validate our findings, we analyzed GSE84437, an independent cohort comprising 433 GC patients (baseline characteristics in Supplementary File 3). Univariate and multivariate Cox regression analysis confirmed that YTHDF2 expression and T3–4 staging were independent prognostic factors, reinforcing the reliability of our observations (Supplementary File 4).

Table 4
Cox regression analysis of prognostic factors for overall survival (OS) after matching.

	HR[a] (95 % CI[b])	P
YTHDF2 expression		
Low	Reference	
High	0.58 (0.37–0.91)	0.018
Age		
≤65	Reference	
>65	1.37 (0.86–2.16)	0.184
Gender		
female	Reference	
male	1.79 (1.05–3.06)	0.034
Stage		
Stage I	Reference	
Stage II	1.32 (0.53–3.30)	0.548
Stage III	2.15 (0.90–5.10)	0.084
Stage IV	3.15 (1.16–8.55)	0.024
Grade		
G1–2	Reference	
G3–4	1.68 (1.04–2.71)	0.034
T		
T1–2	Reference	
T3–4	1.92 (1.05–3.50)	0.033
M		
M0	Reference	
M1	1.29 (0.56–2.98)	0.548
N		
N0	Reference	
N+	1.34 (0.79–2.28)	0.272
Subtype		
MSS[c]	Reference	
MSI-L[d]	1.64 (0.87–3.08)	0.124
MSI-H[e]	0.73 (0.39–1.37)	0.322

[a] HR: hazard ratio;.
[b] 95 % CI: 95 % confidence intervals;.
[c] MSS: microsatellite stability;.
[d] MSI-L: microsatellite instability-low;.
[e] MSI-H: microsatellite instability-high.

YTHDF2 expression and patient survival

To further evaluate the prognostic significance of YTHDF2, we conducted Cox regression analyses across various clinicopathological subgroups of GC patients (Fig. 3). The results indicated that patients younger than 65 years, male patients, those with T3–4 stage, M0 status, N0 status, and MSS subtype had a significantly better prognosis. To further evaluate the prognostic impact of YTHDF2, we conducted Cox regression analyses across various clinicopathological subgroups of GC patients (Fig. 3). The results demonstrated that patients younger than 65 years, male patients, those with T3–4 stage, M0 status, N0 status, and MSS subtype had significantly better overall survival (OS).

Applying propensity score matching (PSM) to balance baseline characteristics between the low- and high-YTHDF2 expression groups at a 1:1 ratio helped minimize potential confounding factors and improve the robustness of our findings. After matching, 212 patients were retained for further analysis (Table 3). An SMD < 0.1 was considered indicative of adequate balance between the matched cohorts.

Subsequent Cox regression analysis in the PSM-adjusted cohort confirmed that high YTHDF2 expression and stage IV disease were independent prognostic factors for OS (Table 4). Kaplan-Meier survival curves further validated that patients with high YTHDF2 expression exhibited significantly better OS, whereas those with stage IV disease had a markedly worse prognosis (Fig. 4A, 4B).

In external validation, patients with higher YTHDF2 expression exhibited significantly improved OS (Supplementary File 5), further reinforcing the prognostic value of YTHDF2 in GC.

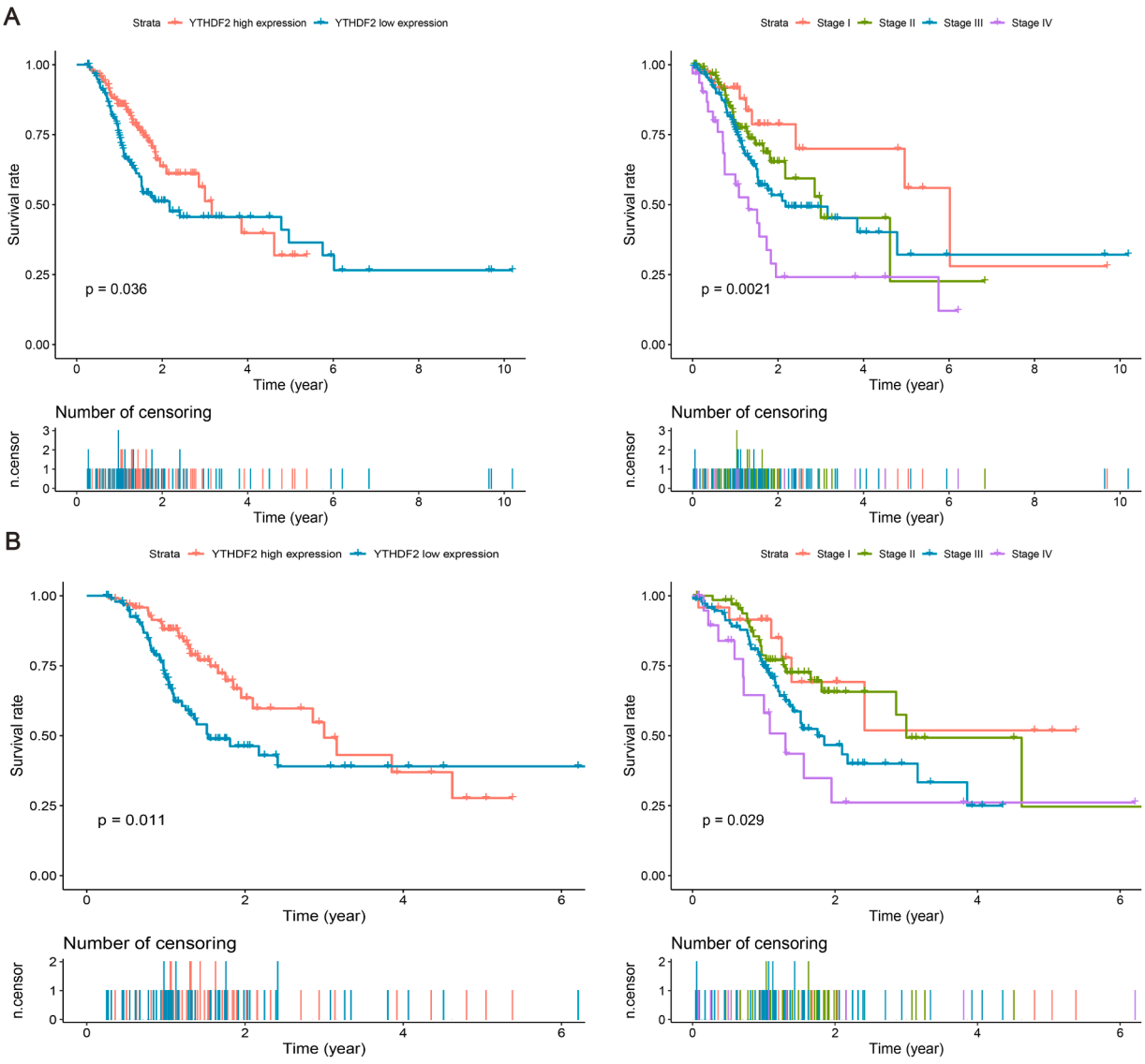

Fig. 4. The survival analysis of YTHDF2 in gastric cancer. The survival analysis between low and high YTHDF2 expression groups before propensity score matching (A) and after propensity score matching (B).

The potential role of YTHDF2 in GC

To elucidate the functional role of YTHDF2 in GC, we performed a differential gene expression analysis between high- and low-YTHDF2 expression groups. A total of 3066 differentially expressed genes (DEGs) were identified using the criteria $|\log_2(\text{Fold Change})| > 1$ and $P < 0.05$ (Supplementary File 6A and 6B).

Gene Ontology (GO) enrichment analysis was conducted to further investigate the biological significance of these DEGs. The results demonstrated that the DEGs were predominantly enriched in biological processes, cellular components, and molecular functions associated with cancer progression and epigenetic regulation. Specifically, the DEGs were significantly involved in histone modification, methylation, methyltransferase complex, histone methyltransferase complex, methyltransferase activity, and p53 binding (Fig. 5A, 5B). These findings suggest that YTHDF2 may play a role in GC through the regulation of epigenetic modifications and tumor suppressor pathways.

Further Kyoto Encyclopedia of Genes and Genomes (KEGG) pathway enrichment analysis revealed that YTHDF2-related DEGs were primarily enriched in several cancer-associated signaling pathways. Notably, these pathways included cell cycle regulation, RNA degradation, mismatch repair, viral carcinogenesis, apoptosis, and the p53 signaling pathway (Fig. 5C, 5D). The involvement of YTHDF2 in these pathways further supports its potential role in GC tumorigenesis and progression.

Overexpression of YTHDF2 inhibits GC cell proliferation and malignancy

To further investigate the biological role of YTHDF2 in GC, RT-qPCR was performed to assess its mRNA expression levels across GC cell lines (HGC27, MKN28, AGS, and SGC7901) and the normal gastric epithelial cell line GES-1. The results demonstrated that YTHDF2 expression was highest in HGC27 cells and lowest in AGS cells (Fig. 6A). Western blot analysis further confirmed that YTHDF2 protein levels were significantly lower in GC cell lines compared to GES-1 (Fig. 6B).

We established YTHDF2 knockdown HGC27 cell lines and YTHDF2-overexpressing AGS cell lines. Colony formation assays revealed that YTHDF2 overexpression markedly suppressed the clonogenic capacity of AGS cells (Fig. 6C), whereas YTHDF2 knockdown significantly enhanced the proliferation of HGC27 cells (Fig. 6D).

Wound healing assays demonstrated that YTHDF2 knockdown reduced the migratory capacity of HGC27 cells (Fig. 6E), whereas YTHDF2 overexpression enhanced the migration ability of AGS cells

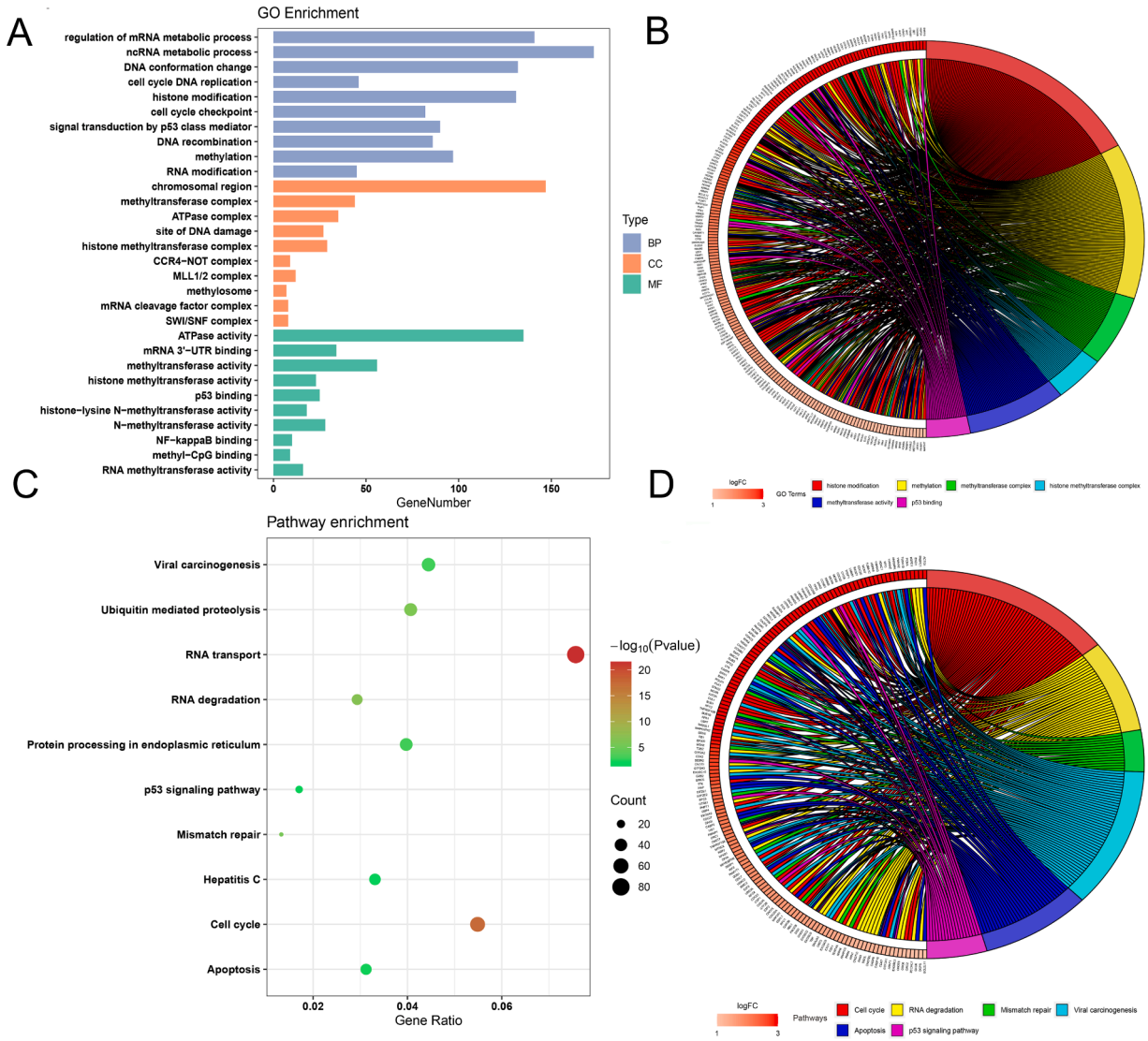

Fig. 5. The potential role and function of YTHDF2-related genes. Functional annotation of the differential expression genes between low and high YTHDF2 expression groups using GO **(A, B)** and KEGG pathway **(C, D)** analysis.

(Fig. 6F). Similarly, Transwell invasion assays showed that YTHDF2 overexpression suppressed the invasive potential of AGS cells (Fig. 7A), while YTHDF2 knockdown promoted the invasion of HGC27 cells (Fig. 7B).

Further investigation into the molecular mechanisms underlying YTHDF2-mediated suppression of GC progression revealed that YTHDF2 overexpression led to a significant reduction in the expression levels of cyclin D1 and cyclin E1, key regulators of cell cycle progression (Fig. 7C). Conversely, YTHDF2 knockdown upregulated cyclin D1 and cyclin E1 expression, reinforcing its role as a potential tumor suppressor (Fig. 7D).

To validate these findings in vivo, tumor xenograft experiments were conducted. Nude mice injected with YTHDF2-overexpressing HGC27 cells exhibited significantly reduced tumor growth and lower tumor weight compared with the control group (Fig. 7D-F). These results collectively indicate that YTHDF2 suppresses GC cell proliferation and malignancy both in vitro and in vivo.

Discussion

RNA m6A modification has emerged as a crucial epigenetic regulator influencing mRNA stability, translation, and degradation, with profound implications for cancer progression [13]. m6A modifications are dynamically regulated by writers (methyltransferases), erasers (demethylases), and readers (m6A-binding proteins) [6,14–18].

Recent studies have highlighted the oncogenic and tumor-suppressive roles of m6A regulators in GC. YTHDF1, another m6A reader, was reported to promote gastric carcinogenesis by facilitating the translation of FZD7, thereby correlating with poor prognosis [19]. Additionally, the m6A writer METTL3 has been implicated in GC progression by modulating downstream oncogenes, activating the MYC signaling pathway, and facilitating epithelial-mesenchymal transition (EMT) [20–24]. Other m6A regulators, including FTO, ALKBH5, WTAP, and KIAA1429, have also been associated with GC progression and patient prognosis [25–27]. However, despite increasing interest in m6A modifications, limited studies have explored the biological function and prognostic role of YTHDF2 in GC.

YTHDF2 has been reported to exert diverse regulatory effects in different cancer types. In hepatocellular carcinoma, it destabilizes EGFR mRNA, suppressing tumor growth [12]. In prostate cancer and osteosarcoma, YTHDF2 plays critical roles in tumor progression and cellular metabolism [28–30]. In this study, we identified YTHDF2 as an independent protective factor for OS in GC patients, with higher YTHDF2 expression correlating with better survival outcomes (HR = 0.58, P =

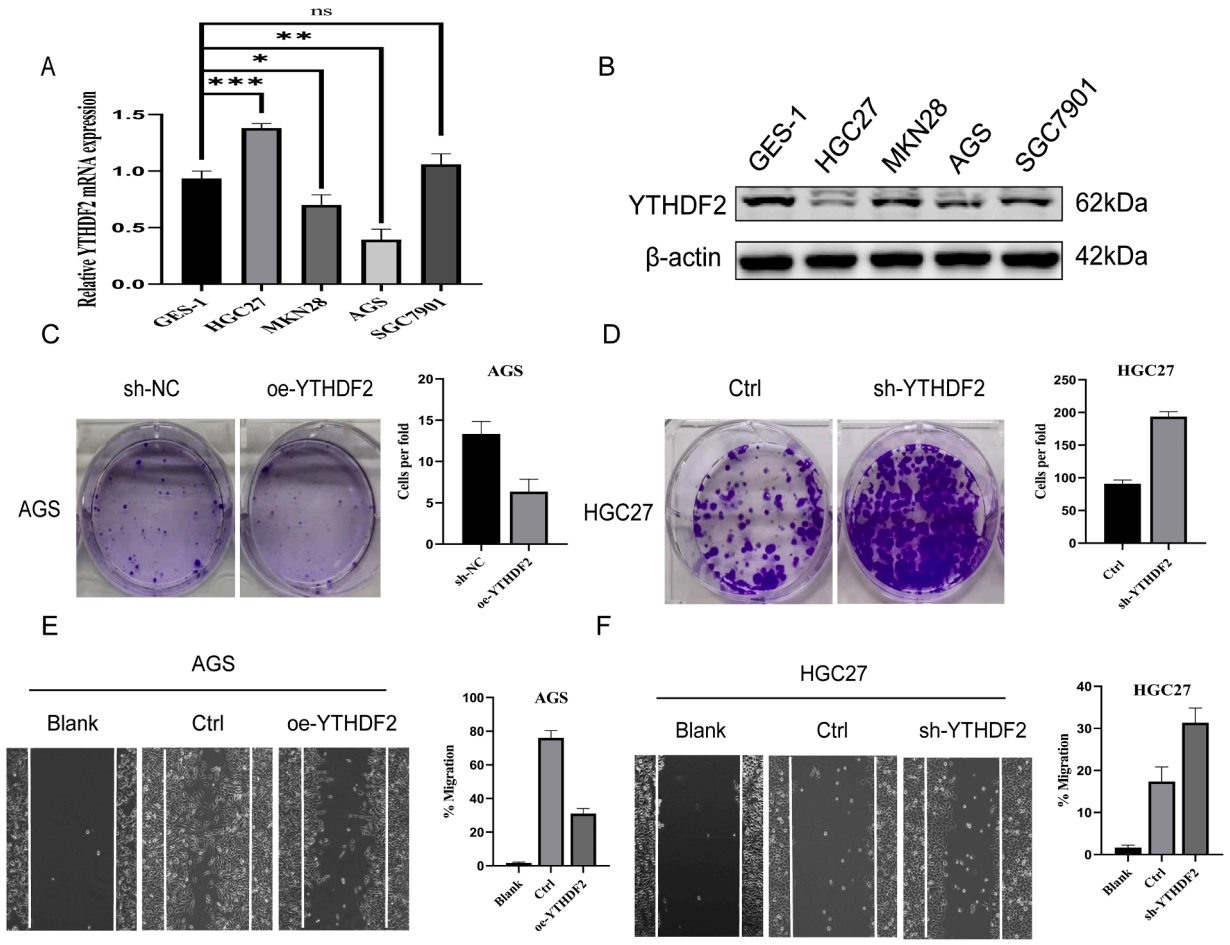

Fig. 6. YTHDF2 inhibits the progression of gastric cancer. **(A, B)** The expression of YTHDF2 was confirmed by qRT-PCR and WB in GES-1, HGC27, MKN28, SGC7901 and AGS cells. **(C, D)** YTHDF2 inhibits colony formation of gastric cancer cells. **(E-F)** Knockdown or overexpression YTHDF2, decreased or increased, respectively, GC cells' wound healing ability in vitro.

0.018). Additionally, tumor stage and patient age were found to be significant predictors of prognosis. However, after PSM adjustment, age was no longer an independent risk factor, while stage IV disease remained strongly associated with poor OS. These findings suggest that while YTHDF2 expression is an important prognostic indicator, tumor burden remains a dominant determinant of patient survival.

Our functional analysis revealed that differentially expressed genes associated with YTHDF2 were significantly enriched in pathways related to methylation, RNA degradation, gene mismatch repair, apoptosis, and p53 signaling. The p53 pathway, a central tumor suppressor network, plays a pivotal role in DNA damage repair, cell cycle arrest, and apoptosis [31]. Recent studies have suggested a regulatory link between YTHDF2 and p53 signaling [32].

For instance, in lung adenocarcinoma, YTHDF2 has been shown to modulate p53 stability by influencing m6A-modified TP53 mRNA decay, thereby regulating the cell cycle and apoptosis [33]. Similarly, in colorectal cancer, YTHDF2 was reported to interact with Mdm2, a key p53 ubiquitin ligase, thereby affecting p53-mediated tumor suppression [34]. Given the enrichment of p53 signaling in our functional analysis, we hypothesize that YTHDF2 may regulate GC progression through its interaction with the p53 pathway, though the precise molecular mechanisms require further investigation.

From a clinical perspective, the identification of YTHDF2 as a prognostic biomarker has potential implications for risk stratification and personalized treatment strategies in GC. Current prognostic models primarily rely on TNM staging, which, while effective, does not account for molecular heterogeneity among patients. Our findings suggest that YTHDF2 expression could serve as an additional prognostic indicator, potentially refining risk assessment beyond conventional staging systems.

However, for YTHDF2 to be translated into routine clinical practice, several factors must be considered. First, the cost-effectiveness of incorporating YTHDF2 assessment into standard diagnostic workflows must be evaluated. Unlike traditional histopathological biomarkers, YTHDF2 requires RNA-based detection methods, such as RT-qPCR or RNA sequencing, which may pose logistical challenges in resource-limited settings. Additionally, prospective clinical studies are needed to validate whether YTHDF2 expression can guide therapeutic decision-making, particularly in the context of targeted therapies or immunotherapy.

Despite these challenges, our study provides compelling evidence that YTHDF2 plays a tumor-suppressive role in GC and has potential clinical utility as a prognostic biomarker. Future research should focus on elucidating its mechanistic role in p53 signaling and evaluating its feasibility as a therapeutic target.

Availability of data and materials

All data generated and analysed during this study are included in this published article.

Ethical statement

The study was approved by Ethical Committee of Shanghai Ninth

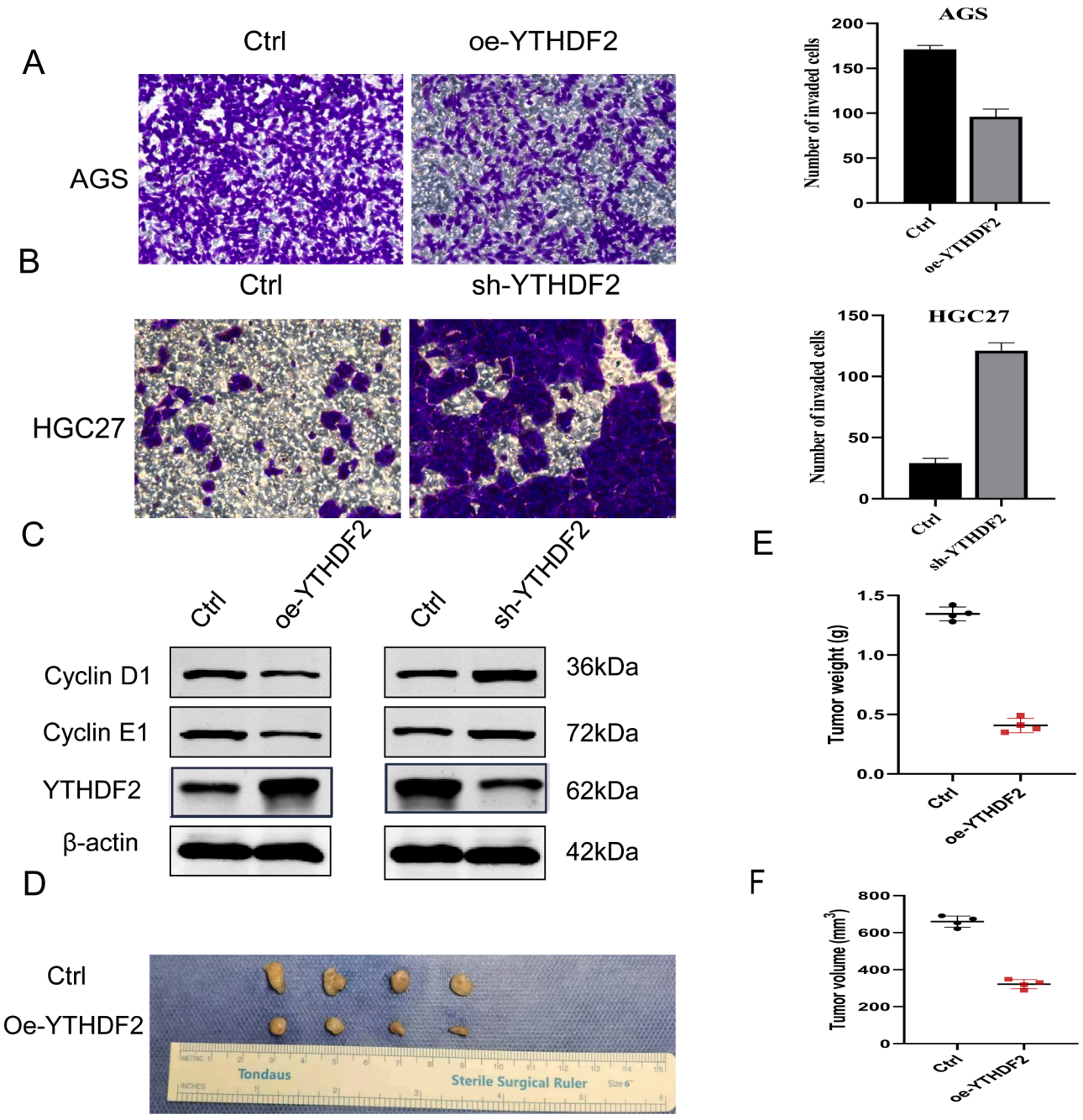

Fig. 7. YTHDF2 inhibits the progression of gastric cancer in vitro and in vivo. **(A, B)** The effect of overexpression or knockout of YTHDF2 on cell invasion. (C) The cell cycle related markers were analyzed by using western blotting with the indicated antibodies. After subcutaneous injection of AGS cells containing a stable overexpression of YTHDF2 or the negative control, photographs of representative tumors were shown **(D)**, tumor volumes were shown **(E)**, The tumor weights **(F)** were measured when the mice were sacrificed and the tumors were excise.

People's Hospital, Shanghai Jiao Tong University School of Medicine.

CRediT authorship contribution statement

Jun Zheng: Writing – original draft, Investigation. **Yinhua Liang:** Visualization, Validation, Resources, Investigation, Writing – original draft, Writing – review & editing. **Xin Xu:** Writing – review & editing, Investigation. **Jianpeng Zhou:** Visualization, Validation, Resources. **Shuang Jiang:** Software, Resources. **Jiwei Yu:** Funding acquisition, Conceptualization.

Declaration of competing interest

The authors declare that they have no known competing financial interests or personal relationships that could have appeared to influence the work reported in this paper.

Funding

Not applicable.

Acknowledgments

We thank the support from Shanghai Ninth People's Hospital, School of Medicine, Shanghai Jiao Tong University and Dr. Chihao Zhang.

Supplementary materials

Supplementary material associated with this article can be found, in the online version, at doi:10.1016/j.tranon.2025.102395.

References

[1] F. Bray, J. Ferlay, I. Soerjomataram, R.L. Siegel, L.A. Torre, A. Jemal, Global cancer statistics 2018: GLOBOCAN estimates of incidence and mortality worldwide for 36 cancers in 185 countries, CA Cancer J. Clin. 68 (6) (2018) 394–424.
[2] E. Van Cutsem, X. Sagaert, B. Topal, K. Haustermans, H. Prenen, Gastric cancer, Lancet 388 (10060) (2016) 2654–2664.
[3] S. Ma, C. Chen, X. Ji, J. Liu, Q. Zhou, G. Wang, et al., The interplay between m6A RNA methylation and noncoding RNA in cancer, J. Hematol. Oncol. 12 (1) (2019) 121.
[4] N. Liu, Q. Dai, G. Zheng, C. He, M. Parisien, T.N. Pan, (6)-methyladenosine-dependent RNA structural switches regulate RNA-protein interactions, Nature 518 (7540) (2015) 560–564.
[5] D.P. Patil, B.F. Pickering, S.R. Jaffrey, Reading m(6)A in the transcriptome: m(6)A-binding proteins, Trends. Cell Biol. 28 (2) (2018) 113–127.
[6] X.Y. Chen, J. Zhang, J.S. Zhu, The role of m(6)A RNA methylation in human cancer, Mol. Cancer 18 (1) (2019) 103.
[7] G. Casella, D. Tsitsipatis, K. Abdelmohsen, Gorospe M. mRNA methylation in cell senescence, Wiley. Interdiscip. Rev. RNa 10 (6) (2019) e1547.
[8] J. Zhou, J. Wan, X. Gao, X. Zhang, S.R. Jaffrey, S.B. Qian, Dynamic m(6)A mRNA methylation directs translational control of heat shock response, Nature 526 (7574) (2015) 591–594.
[9] J. Yan, X. Huang, X. Zhang, Z. Chen, C. Ye, W. Xiang, et al., LncRNA LINC00470 promotes the degradation of PTEN mRNA to facilitate malignant behavior in gastric cancer cells, Biochem. Biophys. Res. Commun. 521 (4) (2020) 887–893.
[10] J. Zhang, J. Pi, Y. Liu, J. Yu, T. Feng, [*Knockdown of YTH N(6)-methyladenosine RNA binding protein 2 (YTHDF2) inhibits proliferation and promotes apoptosis in MGC-803 gastric cancer cells*], Xi. Bao Yu Fen. Zi. Mian. Yi. Xue Za Zhi. 33 (12) (2017) 1628–1634.
[11] J. Chen, Y. Sun, X. Xu, D. Wang, J. He, H. Zhou, et al., YTH domain family 2 orchestrates epithelial-mesenchymal transition/proliferation dichotomy in pancreatic cancer cells, Cell Cycle 16 (23) (2017) 2259–2271.
[12] L. Zhong, D. Liao, M. Zhang, C. Zeng, X. Li, R. Zhang, et al., YTHDF2 suppresses cell proliferation and growth via destabilizing the EGFR mRNA in hepatocellular carcinoma, Cancer Lett. 442 (2019) 252–261.
[13] D. Dominissini, S. Moshitch-Moshkovitz, S. Schwartz, M. Salmon-Divon, L. Ungar, S. Osenberg, et al., Topology of the human and mouse m6A RNA methylomes revealed by m6A-seq, Nature 485 (7397) (2012) 201–206.
[14] K.D. Meyer, Y. Saletore, P. Zumbo, O. Elemento, C.E. Mason, S.R. Jaffrey, Comprehensive analysis of mRNA methylation reveals enrichment in 3′ UTRs and near stop codons, Cell 149 (7) (2012) 1635–1646.
[15] Z. Bodi, A. Bottley, N. Archer, S.T. May, R.G. Fray, Yeast m6A methylated mRNAs are enriched on translating ribosomes during meiosis, and under rapamycin treatment, PLoS. One 10 (7) (2015) e0132090.
[16] T. Csepany, A. Lin, C.J. Baldick Jr., K. Beemon, Sequence specificity of mRNA N6-adenosine methyltransferase, J. Biol. Chem. 265 (33) (1990) 20117–20122.
[17] Y. Wang, Y. Li, M. Yue, J. Wang, S. Kumar, R.J. Wechsler-Reya, et al., N(6)-methyladenosine RNA modification regulates embryonic neural stem cell self-renewal through histone modifications, Nat. Neurosci. 21 (2) (2018) 195–206.
[18] B. Xie, Z. Deng, Y. Pan, C. Fu, S. Fan, Y. Tao, et al., Post-transcriptional regulation DPC4 gene by miR-190 in colorectal cancer cells, J. Cancer Res. Ther. 14 (4) (2018) 838–843.
[19] J. Pi, W. Wang, M. Ji, X. Wang, X. Wei, J. Jin, et al., YTHDF1 promotes gastric carcinogenesis by controlling translation of FZD7, Cancer Res. (2020).
[20] L. Jiang, T. Chen, L. Xiong, J.H. Xu, A.Y. Gong, B. Dai, et al., Knockdown of m6A methyltransferase METTL3 in gastric cancer cells results in suppression of cell proliferation, Oncol. Lett. 20 (3) (2020) 2191–2198.
[21] J.W. Xie, X.B. Huang, Q.Y. Chen, Y.B. Ma, Y.J. Zhao, L.C. Liu, et al., m(6)A modification-mediated BATF2 acts as a tumor suppressor in gastric cancer through inhibition of ERK signaling, Mol. Cancer 19 (1) (2020) 114.
[22] D.D. Yang, Z.H. Chen, K. Yu, J.H. Lu, Q.N. Wu, Y. Wang, et al., METTL3 Promotes the progression of gastric cancer via targeting the MYC pathway, Front. Oncol. 10 (2020) 115.
[23] B. Yue, C. Song, L. Yang, R. Cui, X. Cheng, Z. Zhang, et al., METTL3-mediated N6-methyladenosine modification is critical for epithelial-mesenchymal transition and metastasis of gastric cancer, Mol. Cancer 18 (1) (2019) 142.
[24] H. He, W. Wu, Z. Sun, L. Chai, MiR-4429 prevented gastric cancer progression through targeting METTL3 to inhibit m(6)A-caused stabilization of SEC62, Biochem. Biophys. Res. Commun. 517 (4) (2019) 581–587.
[25] Y. Li, D. Zheng, F. Wang, Y. Xu, H. Yu, H. Zhang, Expression of demethylase genes, FTO and ALKBH1, is associated with prognosis of gastric cancer, Dig. Dis. Sci. 64 (6) (2019) 1503–1513.
[26] H. Li, Q. Su, B. Li, L. Lan, C. Wang, W. Li, et al., High expression of WTAP leads to poor prognosis of gastric cancer by influencing tumour-associated T lymphocyte infiltration, J. Cell Mol. Med. 24 (8) (2020) 4452–4465.
[27] R. Miao, C.C. Dai, L. Mei, J. Xu, S.W. Sun, Y.L. Xing, et al., KIAA1429 regulates cell proliferation by targeting c-Jun messenger RNA directly in gastric cancer, J. Cell Physiol. 235 (10) (2020) 7420–7432.
[28] X. Wu, X. Zhang, L. Tao, X. Dai, P. Chen, Prognostic value of an m6A RNA methylation regulator-based signature in patients with hepatocellular carcinoma, Biomed. Res. Int. 2020 (2020) 2053902.
[29] J. Wang, H. Lin, M. Zhou, Q. Xiang, Y. Deng, L. Luo, et al., The m6A methylation regulator-based signature for predicting the prognosis of prostate cancer, Fut. Oncol. (2020).
[30] J. Li, B. Rao, J. Yang, L. Liu, M. Huang, X. Liu, et al., Dysregulated m6A-related regulators are associated with tumor metastasis and poor prognosis in osteosarcoma, Front. Oncol. 10 (2020) 769.
[31] B.S. Lapa, M.I. Costa, D. Figueiredo, J. Jorge, R. Alves, A.R. Monteiro, et al., AZD-7648, a DNA-PK inhibitor, induces DNA damage, apoptosis, and cell cycle arrest in chronic and acute myeloid leukemia cells, Int. J. Mol. Sci. 24 (20) (2023).
[32] Guo X., Li K., Jiang W., et al. RNA demethylase ALKBH5 prevents pancreatic cancer progression by posttranscriptional activation of PER1 in an m6A-YTHDF2-dependent manner.
[33] N.I. Vokes, E. Chambers, T. Nguyen, A. Coolidge, C.A. Lydon, X. Le, et al., Concurrent TP53 mutations facilitate resistance evolution in EGFR-mutant lung adenocarcinoma, J. Thorac. Oncol. 17 (6) (2022) 779–792.
[34] F.Y. Zhang, L. Wu, T.N. Zhang, H.H. Chen, KCTD15 acts as an anti-tumor factor in colorectal cancer cells downstream of the demethylase FTO and the m6A reader YTHDF2, Commun. Biol. 7 (1) (2024) 262.